



Defence Research and
Development Canada

Recherche et développement
pour la défense Canada



Noise Radar Technology Basics

T. Thayaparan and C. Wernik

Defence R&D Canada – Ottawa

TECHNICAL MEMORANDUM

DRDC Ottawa TM 2006-266

December 2006

Canada

Report Documentation Page				Form Approved OMB No. 0704-0188	
Public reporting burden for the collection of information is estimated to average 1 hour per response, including the time for reviewing instructions, searching existing data sources, gathering and maintaining the data needed, and completing and reviewing the collection of information. Send comments regarding this burden estimate or any other aspect of this collection of information, including suggestions for reducing this burden, to Washington Headquarters Services, Directorate for Information Operations and Reports, 1215 Jefferson Davis Highway, Suite 1204, Arlington VA 22202-4302. Respondents should be aware that notwithstanding any other provision of law, no person shall be subject to a penalty for failing to comply with a collection of information if it does not display a currently valid OMB control number.					
1. REPORT DATE DEC 2006		2. REPORT TYPE N/A		3. DATES COVERED -	
4. TITLE AND SUBTITLE Noise Radar Technology Basics				5a. CONTRACT NUMBER	
				5b. GRANT NUMBER	
				5c. PROGRAM ELEMENT NUMBER	
6. AUTHOR(S)				5d. PROJECT NUMBER	
				5e. TASK NUMBER	
				5f. WORK UNIT NUMBER	
7. PERFORMING ORGANIZATION NAME(S) AND ADDRESS(ES) Defence R&D Canada - Ottawa Technical Memorandum DRDC Ottawa TM 2006-266 Canada				8. PERFORMING ORGANIZATION REPORT NUMBER	
9. SPONSORING/MONITORING AGENCY NAME(S) AND ADDRESS(ES)				10. SPONSOR/MONITOR'S ACRONYM(S)	
				11. SPONSOR/MONITOR'S REPORT NUMBER(S)	
12. DISTRIBUTION/AVAILABILITY STATEMENT Approved for public release, distribution unlimited					
13. SUPPLEMENTARY NOTES The original document contains color images.					
14. ABSTRACT					
15. SUBJECT TERMS					
16. SECURITY CLASSIFICATION OF:			17. LIMITATION OF ABSTRACT SAR	18. NUMBER OF PAGES 52	19a. NAME OF RESPONSIBLE PERSON
a. REPORT unclassified	b. ABSTRACT unclassified	c. THIS PAGE unclassified			

Noise Radar Technology Basics

T. Thayaparan
Defence R&D Canada – Ottawa

C. Wernik
Carleton University

Defence R&D Canada – Ottawa

Technical Memorandum

DRDC Ottawa TM 2006-266

December 2006

Principal Author

Original signed by T. Thayaparan

T. Thayaparan

Approved by

Original signed by Aaron Spaans

Aaron Spaans

Acting Head/RAST Section

Approved for release by

Original signed by Cam Boulet

Cam Boulet

Head/Document Review Panel

© Her Majesty the Queen in Right of Canada as represented by the Minister of National Defence, 2006

© Sa Majesté la Reine (en droit du Canada), telle que représentée par le ministre de la Défense nationale, 2006

Abstract

Recently, there has been considerable interest in noise radar over a wide spectrum of applications, such as through wall surveillance, detection, tracking, Doppler estimation, polarimetry, interferometry, ground-penetrating or subsurface profiling, synthetic aperture radar (SAR) imaging, inverse synthetic aperture radar (ISAR) imaging, foliage penetration imaging, etc. One of the major advantages of the noise radar is its inherent immunity from jamming, detection, and external interference. In this report, the basic theory of noise radar design is treated. The theory supports the use of noise waveforms for radar detection and imaging in such applications as covert military surveillance and reconnaissance. It is shown that by using wide-band noise waveforms, one can achieve high resolution and reduced ambiguities in range and Doppler estimations. Two coherent processing receivers, namely, the correlation receiver and the double spectral processing receiver of noise radar returns are described and their range estimation is presented. Mutual interference and low probability of interception (LPI) capabilities of noise radar are also evaluated. The simulation results show the usefulness of the noise radar technology to improve on conventional radars.

Résumé

Récemment, le radar à bruit a suscité un intérêt considérable aux fins d'un large éventail d'applications, p. ex. surveillance à travers les murs, poursuite, estimation Doppler, polarimétrie, interférométrie, sondage du sol ou profilage de la sous-surface, détection, imagerie SAR (radar à synthèse d'ouverture) et ISAR (radar à synthèse d'ouverture inverse) et imagerie par pénétration du feuillage. Un de ses grands avantages est son immunité au brouillage intentionnel, à la détection et au brouillage externe. Le présent rapport aborde les principes de base du radar à bruit, qui soutiennent l'utilisation de formes d'onde de bruit pour la détection et l'imagerie radar dans des applications telles que la surveillance et la reconnaissance militaires secrètes. Nous montrons que l'utilisation de formes d'onde à large bande permet une haute résolution et la réduction des ambiguïtés de mesure de distance et d'estimation Doppler. Deux récepteurs de traitement cohérent, soit le récepteur de corrélation et le récepteur de traitement DSP (traitement spectral double) des échos radar sont décrits et une estimation de leur portée est présentée. Les capacités LPI (faible probabilité d'interception) et de brouillage réciproque du radar à bruit sont également évaluées. Les résultats des simulations montrent l'utilité du radar à bruit, qui améliore les capacités des radars classiques.

This page intentionally left blank.

Executive summary

Noise Radar Technology Basics

T. Thayaparan, C. Wernik; DRDC Ottawa TM 2006-266; Defence R&D Canada – Ottawa; December 2006.

Target detection, identification, imaging and tracking are all essential operations in military radar applications. They must be carried out in a variety of difficult conditions and environments that may include high target density, dense clutter and jamming. This report proposes the use of noise radar systems for successful execution of the above operations in such environments.

Noise radar is a form of random signal radar whose transmitting signal is a microwave noise source or is modulated by a lower frequency white noise source in contrast to the conventional pulse, CW (continuous wave), FM (frequency modulated), or FM/CW radars. Because of the truly random transmitting signal, noise radars have many advantages compared with conventional radars, including unambiguous measurement of range and Doppler estimations, high immunity to noise, very low probability of intercept (LPI), high electro-magnetic compatibility, good electronic counter countermeasure (ECCM) capability, good counter electronic support measure (CESM) capability, and ideal 'thumbtack' ambiguity function. Thus, as soon as the concept of noise radar appeared, many people paid close attention and many studies emerged. The earliest research work related to noise radar occurred about 45 years ago, but since techniques of that time were immature, noise radar development proceeded slowly. Part of the reason was due to the limited availability of suitable electronic components. Now, along with progress of digital signal processing algorithms, signal processing hardware, solid state microwave components and high-speed VLSI (very large scale integration), the realization of noise radar was relatively easy. On the other hand, owing to the electronic jamming in modern war, much more attention is paid to noise radar because of its good ECCM and CESM properties.

This report evaluates the noise radar basics. We describe two signal processing techniques of noise radar returns. One of them uses the correlation processing of the radar returns, while the second one exploits their, so-called, double spectral processing. Both methods combine the transmitted and received noise waveforms in such a way that the range to the target can be determined. Simulation results show that both methods unambiguously determine the range of the target. We evaluate the mutual interference effects on noise radars and linear frequency modulated (LFM) waveform radars caused by other radars when determining the range and velocity of a moving target. The results show that noise radars, because of the random nature of the waveforms, are very good at suppressing very high level interference from other radars compared to LFM radars. An evaluation of the probability that the noise

radar's noise waveform would be detected is also studied. It is shown that in a variety of noisy environments, the noise radar always has a much lower LPI than the conventional LFM radar. The noise radar's exceptional performance in the above evaluations makes it a suitable radar system for a variety of military applications.

It is recommended that the exploitation of noise radar, as a highly advanced military surveillance and reconnaissance radar system, be undertaken to improve battlefield operations. We identify specific cases that are common in today's Canadian Forces' deployment areas where noise radar would be crucial in addressing hostile threats, specially in the area of through wall surveillance, ground-penetrating or subsurface probing applications, and foliage penetration (FOPEN) applications.

Sommaire

Noise Radar Technology Basics

T. Thayaparan, C. Wernik; DRDC Ottawa TM 2006-266; R & D pour la défense Canada – Ottawa; décembre 2006.

La détection, l'identification, l'imagerie et la poursuite de cibles sont des opérations essentielles des applications radar militaires. Elles doivent être menées dans diverses conditions et environnements difficiles, p. ex. haute densité de cibles, clutter dense et brouillage intentionnel. Le présent rapport propose l'utilisation de systèmes radar à bruit pour l'exécution efficace de ces opérations dans de tels environnements.

Le radar à bruit est un radar à signal aléatoire qui émet un bruit hyperfréquence ou un signal modulé par une source de bruit blanc de fréquence plus basse, contrairement aux radars classiques à impulsions, à onde entretenue (CM), à modulation de fréquence (FM) ou FM/CW. Étant donné son signal véritablement aléatoire, le radar à bruit offre bien des avantages par rapport aux radars classiques, p. ex. mesure non ambiguë de la distance et de l'estimation Doppler, grande immunité au bruit, très faible probabilité d'interception (LPI), grande compatibilité électromagnétique, bonne capacité de contre-mesures électroniques (CCME) et de contre-mesures de soutien électronique (CESM) et fonction d'ambiguïté en pointe idéale. Ainsi, dès que le concept de radar à bruit est apparu, de nombreuses personnes s'y sont intéressées de près et un grand nombre d'études ont été réalisées. Les premiers travaux remontent à près de 45 ans, mais comme les techniques étaient alors peu développées, l'évolution a été lente, en partie à cause de la rareté des composants électroniques nécessaires. Avec l'évolution des algorithmes de traitement numérique des signaux, du matériel de traitement des signaux, des composants hyperfréquences à semiconducteurs et de la technologie VLSI (intégration à très grande échelle) haute vitesse, la réalisation du radar à bruit est aujourd'hui relativement aisée. D'autre part, compte tenu de l'utilisation du brouillage électronique intentionnel dans la guerre moderne, le radar à bruit suscite un intérêt encore plus grand étant donné ses bonnes propriétés CCME et CESM.

Le présent rapport évalue les principes de base du radar à bruit. Il décrit deux techniques de traitement des échos de ce radar. L'une utilise le traitement par corrélation des échos des radars, et l'autre la technique DSP (traitement spectral double). Les deux méthodes combinent les formes d'onde de bruit émises et reçues afin de déterminer la distance de la cible. Les résultats des simulations montrent que les deux méthodes déterminent sans ambiguïté la distance de la cible. Nous évaluons les effets de brouillage réciproque sur les radars à bruit et les radars à forme d'onde LFM (modulation linéaire de la fréquence), causés par d'autres radars, lors de la détermination de la distance et de la vitesse d'une cible mobile. Les résultats montrent qu'en raison

de la nature aléatoire des formes d'onde, les radars à bruit sont très efficaces pour supprimer le brouillage de très haut niveau provenant d'autres radars, par rapport aux radars LFM. Une évaluation de la probabilité de détection de leur forme d'onde est également étudiée. Le rapport montre que dans divers milieux bruyants, le radar à bruit a toujours une LPI très inférieure à celle d'un radar LFM classique. Ses performances exceptionnelles lors des évaluations en font un système radar bien adapté à diverses applications militaires.

L'exploitation du radar à bruit, comme système radar militaire de surveillance et de reconnaissance hautement perfectionné, est recommandée afin d'améliorer les opérations tactiques. Nous identifions certains cas aujourd'hui communs dans les zones de déploiement des Forces canadiennes où le radar à bruit serait d'une importance cruciale face à des menaces ennemies, en particulier pour la surveillance à travers les murs, le sondage du sol ou de la sous-surface et la pénétration du feuillage (FOPEN).

Table of contents

Abstract	i
Résumé	i
Executive summary	iii
Sommaire	v
Table of contents	vii
List of figures	viii
1 Introduction	1
2 Noise Radar Basics	3
2.1 Correlation Receiver	3
2.1.1 Correlation Receiver Simulation	6
2.2 Double Spectral Processing Receiver	8
2.2.1 Double Spectral Processing Receiver Simulation	9
2.3 Mutual Interference	10
2.3.1 Mutual Interference Simulation	10
2.3.2 Comparison Between noise radar and Conventional LFM Radar	12
2.4 Probability of Interception	23
3 Discussion and Conclusion	27
3.1 Through wall surveillance	27
3.2 Random noise polarimetry for high-resolution subsurface probing applications	28
3.3 Random noise polarimetry for high-resolution foliage penetration applications	28
References	30

List of figures

Figure 1:	Main components of noise radar with external delay line.	4
Figure 2:	Correlation receiver example (three targets located at $r_1 = 100$ m, $r_2 = 400$ m and $r_3 = 500$ m).	7
Figure 3:	Double spectral processing receiver example (single target at $r_0 = 100$ m)	9
Figure 4:	Location of three radars	11
Figure 5:	Range-Doppler profiles. Radars operate with the same transmit power. Upper row: radar returns of the first, second and third radars without MI. Lower row: radar returns of the first, second and third radars with MI.	13
Figure 6:	Range-Doppler profiles. Radars operate with the following relative transmit powers: +20 dB, +3 dB and 0 dB. Upper row: radar returns of the first, second and third radars without MI. Lower row: radar returns of the first, second and third radars with MI.	14
Figure 7:	Range-Doppler profiles. Radars operate with the following relative transmit powers: +30 dB, +3 dB and 0 dB. Upper row: radar returns of the first, second and third radars without MI. Lower row: radar returns of the first, second and third radars with MI.	15
Figure 8:	Range-Doppler profiles. Radars operate with the following relative transmit powers: +35 dB, +3 dB and 0 dB. Upper row: radar returns of the first, second and third radars without MI. Lower row: radar returns of the first, second and third radars with MI.	16
Figure 9:	Range-Doppler profiles. Radars operate with the following relative transmit powers: +40 dB, +3 dB and 0 dB. Upper row: radar returns of the first, second and third radars without MI. Lower row: radar returns of the first, second and third radars with MI.	17
Figure 10:	Conventional LFM radars. Three radars are considered. Subplots on the left side present range-Doppler profiles when the radars operate without interference. Subplots on the right side show interference effects when the radars operate simultaneously. The second radar's transmit power is 12 dB higher than the transmit powers of the first and third radars.	19

Figure 11:	Random waveform radars. Three radars are considered. Subplots on the left side present range-Doppler profiles when the radars operate without interference. Subplots on the right side show interference effects when the radars operate simultaneously. The second radar's transmit power is 12 dB higher than the transmit power of the first and third radars.	20
Figure 12:	Conventional LFM radars. Three radars are considered. Subplots on the left side present range-Doppler profiles when the radars operate without interference. Subplots on the right side show interference effects when the radars operate simultaneously. All radars operate with same transmit power.	21
Figure 13:	Random waveform radars. Three radars are considered. Subplots on the left side present range-Doppler profiles when the radars operate without interference. Subplots on the right side show interference effects when the radars operate simultaneously. All three radars operate with the same transmit power.	22
Figure 14:	Fourier spectrum of the observed signal in the case of a conventional LFM radar (left) and a NR (right) for various observation times. N_p is the number of radar pulses within the observation time. The signal to noise ratio is 10 dB.	24
Figure 15:	Fourier spectrum of the observed signal in the case of a conventional LFM radar (left) and a NR (right) for various observation times. N_p is the number of radar pulses within the observation time. The signal to noise ratio is 0 dB.	25
Figure 16:	Fourier spectrum of the observed signal in the case of a conventional LFM radar (left) and a NR (right) for various observation times. N_p is the number of radar pulses within the observation time. The signal to noise ratio is -6 dB.	26

This page intentionally left blank.

1 Introduction

Noise radar is a form of random signal radar that employs a noise waveform as the transmitted signal and uses coherent processing of radar returns in contrast to the conventional pulse, CW (continuous wave), FM (frequency modulated), or FM/CW radars. Because of the truly random transmitting signal, noise radars have many advantages compared with conventional radars, including unambiguous measurement of range and Doppler estimations, high immunity to noise, low probability of intercept (LPI), high electro-magnetic compatibility, good electronic counter countermeasure (ECCM) capability, good counter electronic support measure (CESM) capability, very low probability of intercept (LPI), and ideal 'thumbtack' ambiguity function [1]-[25]. Noise radar systems have not yet reached sufficient maturity for military use. The objective of this report is to make clear the advantageous properties of noise radar in current and for future military applications.

The research on noise radar or random signal radar started during the 1960s [5]. At that time, theoretical analysis was made and some prototypes were constructed. However, due to the limited availability of suitable electronic components, the research on noise radar dropped quickly, for the following reasons: 1) while generation of pseudorandom signal has been well developed, generation of pure random signal was much more difficult; 2) for noise radar, modulation of a transmitting signal is random. So the correlation processing is necessary instead of the common pulse compressor. Therefore, microwave variable delay-line is a key component in the receiver of noise radar. However, the manufacturing of microwave variable delay-line was also very difficult to do in the past. Since the 1990s, with the development of solid-state microwave components and high-speed VLSI (very large scale integration), enabling the generation of a microwave random signal and manufacture of microwave variable delay-line. This technical progress most likely ensures the implementation of noise radar soon. Thus, the research on noise radar has become more and more required. An all-around review of noise radar or random signal radar in the past thirty years are given in [11]-[12].

Over the past few years, the research has been devoted to the development and implementation of random noise radar by various research groups [8], [4], [13]-[17]. Recent research has investigated the potential use of noise radar for ultrawideband SAR/ISAR imaging, Doppler and polarimetric measurements, collision warning, detection of buried objects, and targets obscured by foliage [2], [6], [15]-[25]. Wide bandwidth gives high range resolution, and the extended pulse length improves the transmitted average power. The non-periodic waveform suppresses the range ambiguity while reducing the probability of intercept and interference. The implementations of varying complexity of noise radar were analyzed and discussed in [1]-[25].

In this report, we describe two methods for coherent processing of noise radar returns.

In both cases, a part of the transmitted signal is used as a reference. When a radar return is received, it is down converted to the IF-band coherently using the reference signal. How those signals are used next depends on the method used. The first is correlation reception. This method makes use of a digital delay line to delay the reference signal before multiplying it by the IF radar return. The resulting product is passed through a low pass filter to produce a correlation function of the product. The range of a target is estimated as the time delay given by the position of the correlation function's maximum [1]-[2], [4], [6]. We derive correlation functions for such a receiver based on a variety of transmitted signals and present results from simulations of specific radar systems. The second method for coherent processing of noise radar returns is double spectral processing reception [10]. Also known as the spectral interferometry method, the double spectral processing is another way of estimating a target's range. The simplest implementation of such a receiver adds the reference and radar return before converting them down to the IF-band. The sum is then fitted into a spectrum analyzer and the time delay is determined via the Fourier transform of the resulting power spectrum [2]. We will derive the power spectrum of the sum of arbitrary signals via its autocorrelation function. We also show how to extract the time delay based on the position of the maxima in the Fourier transform. A simulation of a noise radar system consisting of a double spectral processing receiver is presented.

An important operational consideration of all radar systems is mutual interference. We examine the case when multiple noise radars are operating simultaneously in order to provide results concerning mutual interference operation. These results are compared to those obtained by conventional radars employing a linear frequency modulated (LFM) waveform. Also, more specific to the application of covert surveillance, is the low probability of interception performance of radar systems. In this report, we compare noise radars with conventional LFM radars in terms of the ability to detect either one in various noisy environments.

This report is focused on presenting basic principles of noise radar technology. Significant improvements in military systems may be realized in radio frequency application areas by taking advantage of emergent noise radar technology for advanced radar design. This technology can lead to sophisticated surveillance and reconnaissance techniques through the ability to overcome hostile CESMs and other threats.

2 Noise Radar Basics

2.1 Correlation Receiver

The correlation uses the principle that when the delayed reference signal is correlated with the actual target echo, the peak value of the correlation process can indicate the distance to the target (the amount of time delay of the reference signal is also a measure of distance to the target), while outputs of Doppler filters following the correlator give target velocity [8]. Figure 1 shows the main elements of random noise radar. A noise signal is transmitted, and a delayed signal is received from a point target. A replica of the transmitted noise, delayed by T_0 , is correlated with the received signal. When T_r is varied a strong correlation peak is obtained for $T_r = T_0$, which gives an estimate of the target range $r_0 = cT_0/2$.

Let us consider a radar emitting a time limited signal $x(t)$. Denote the received signal by $y(t)$. Furthermore, we assume that a single point scatterer is located at the range r_0 along the radar line-of-sight (LOS). According to this assumption, the received signal can be written as:

$$y(t) = A_\sigma x(t - T_0) + \varepsilon(t) \quad (1)$$

where $T_0 = 2r_0/c$ is the round-trip delay caused by the finite speed of the electromagnetic waves, $\varepsilon(t)$ is an undesired part of the received signal (noise caused by the reflection from other objects along the LOS) and A_σ denotes target reflectivity. Without loss of generality we will assume that $A_\sigma = 1$. The correlation of the emitted and received signals can be written as:

$$R(\tau) = \int_0^{T_{int}} y(t)x^*(t - \tau)dt. \quad (2)$$

where T_{int} is the integration time. In the noiseless case, the maximum value of $|R(\tau)|$ is at the point $\tau = T_0$.

In the case of conventional radars, the signal $x(t)$ can be expressed as:

$$x(t) = A(t)e^{j\varphi(t)} \quad (3)$$

where the amplitude $A(t)$ and the instantaneous frequency $\omega(t) = \varphi'(t)$ are continuous, slow-varying functions. The integrand in (2) is of the form:

$$\begin{aligned} y(t)x^*(t - \tau) &= A(t - T_0)A^*(t - \tau)e^{j\varphi(t - T_0) - j\varphi(t - \tau)} \\ &\approx |A(t)|^2 e^{j\omega(t)(\tau - T_0)} \end{aligned} \quad (4)$$

Furthermore if the radar emits a LFM signal with constant amplitude $A(t) = A_0$, $\omega(t) = \omega_0 + at$ we get:

$$y(t)x^*(t - \tau) = |A_0|^2 e^{j\omega_0(\tau - T_0)} e^{jat(\tau - T_0)} \quad (5)$$

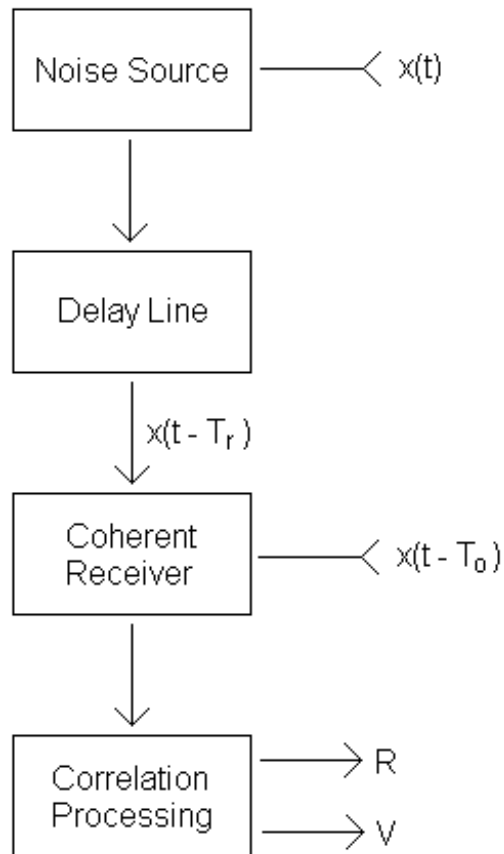


Figure 1: Main components of noise radar with external delay line.

and

$$\begin{aligned}
R(\tau) &= |A_0|^2 e^{j\omega_0(\tau-T_0)} \int_0^{T_{int}} e^{jat(\tau-T_0)} dt \\
&= |A_0|^2 e^{j\omega_0(\tau-T_0)} \frac{1}{ja(\tau-T_0)} (e^{jaT_{int}(\tau-T_0)} - 1) \\
&= |A_0|^2 e^{j\omega_0\tau - jaT_{int}(\tau-T_0)/2} \cdot 2 \frac{\sin(a(\tau-T_0)T_{int}/2)}{a(\tau-T_0)}
\end{aligned} \tag{6}$$

Once again, the maximal value of $|R(\tau)|$ is at $\tau = T_0$.

Let us now assume that $x(t)$ is a white stationary Gaussian random process with autocorrelation function $R_{xx}(\tau)$. The output of the correlation receiver given by (2) is also a random process. Let us analyze the expected value of (2) as:

$$\begin{aligned}
E[R(\tau)] &= E\left[\int_0^{T_{int}} y(t)x^*(t-\tau)dt\right] \\
&= \int_0^{T_{int}} E[y(t)x^*(t-\tau)]dt \\
&= \int_0^{T_{int}} E[x(t-T_0)x^*(t-\tau)] + E[\varepsilon(t)x^*(t-\tau)]dt \\
&= \int_0^{T_{int}} R_{xx}(\tau-T_0)dt + \int_0^{T_{int}} E[\varepsilon(t)x^*(t-\tau)]dt
\end{aligned} \tag{7}$$

If the emitted signal $x(t)$ and the noise $\varepsilon(t)$ are independent processes then the second term in (7) is equal to zero and we get:

$$E[R(\tau)] = T_{int} R_{xx}(\tau - T_0). \tag{8}$$

Since the autocorrelation function's maximum is at $u = 0$ ($R(\tau) \leq R(0)$), the delay T_0 can be estimated as the position of the maximum as:

$$T_0 = \max_{\tau} |E[R(\tau)]| \tag{9}$$

Special cases:

- Let $x(t)$ be the white stationary Gaussian random process. The autocorrelation function is $R_{xx}(\tau) = I_0\delta(t-\tau)$. This is an ideal shape since $E[R(\tau)] = T_{int}I_0\delta(t-\tau)$, and its maxima are ideally defined (only one point is different from zero). Note that signals of this form are not bandlimited and they can not be used in practical applications.

- Let $x(t)$ be the bandlimited white stationary Gaussian random process with power spectral density (PSD) $S_{xx}(f) = S_0$ for $f_0 - B/2 \leq f < f_0 + B/2$ and $S_{xx}(f) = 0$ otherwise. The autocorrelation function is of the form:

$$R_{xx}(\tau) = S_0 e^{j2\pi f_0 \tau} \frac{\sin(\pi B \tau)}{\pi \tau} \quad (10)$$

with well defined maxima at $\tau = 0$, but also with side lobes. The first side lobe is $B \frac{\pi}{2}$ times lower than the main maximum.

2.1.1 Correlation Receiver Simulation

Let us assume that the transmitted and received signals are demodulated to the baseband $-B/2 \leq f < B/2$. In this case, according to the sampling theorem, we must have $N = BT_{int}$ samples within one pulse. $x(n)$ denotes the samples of the transmitted signal and $y(n)$ denotes the samples of the received signal. Then we can calculate the correlation in the discrete domain as:

$$R(k) = \sum_{n=0}^{N-1} y(n)x^*(n-k) \quad (11)$$

and the maximum of $R(\tau)$ is estimated with discretization step $\Delta\tau = \frac{T_{int}}{N} = \frac{1}{B}$ and the range resolution will be $\Delta r = \frac{c}{2B}$, as in the case of conventional radars.

Note that the number of range cells, i.e. the range of the index k in (11) can be less than N . Namely if we define the maximum target range r_{\max} then we should use $k = 0, 1, \dots, k_{\max}$, and $k_{\max} = \frac{r_{\max}}{\Delta r} = N \frac{2r_{\max}}{T_{int}c}$ can be significantly less than N . In this way we can significantly reduce the computational burden associated with the correlation receiver, which in turn can strengthen its usefulness in an operational situation for short-range applications.

The fast Fourier transform (*FFT*) can be used for the calculation (11)

$$R(k) = FFT^{-1}[FFT[y(n)]FFT^*[x(n)]] \quad (12)$$

Note that in this case we obtain N samples of $R(\tau)$, so if $k_{\max} \ll N$ we will have many unnecessary calculations.

In this simulation we use the radar carrier frequency $f_0 = 10$ GHz, bandwidth $B = 51.2$ MHz, and pulse repetition frequency PRF = 1000 kHz. The number of samples within the radar pulse is $N = BT_{int} = 512$. The range resolution is $\Delta r = \frac{c}{2B} = 2.93$ m, and the maximum range is $r_{\max} = N\Delta r = 1500$ m. There are three stationary targets simulated along the LOS at $r_1 = 100$ m, $r_2 = 400$ m and $r_3 = 500$ m. The correlation $R(k)$ is calculated according to the equation (11) and the results are presented in Figure 2. Figure 2 clearly shows that there are three strong correlation peaks located at the expected ranges. Note that there are no sidelobes.

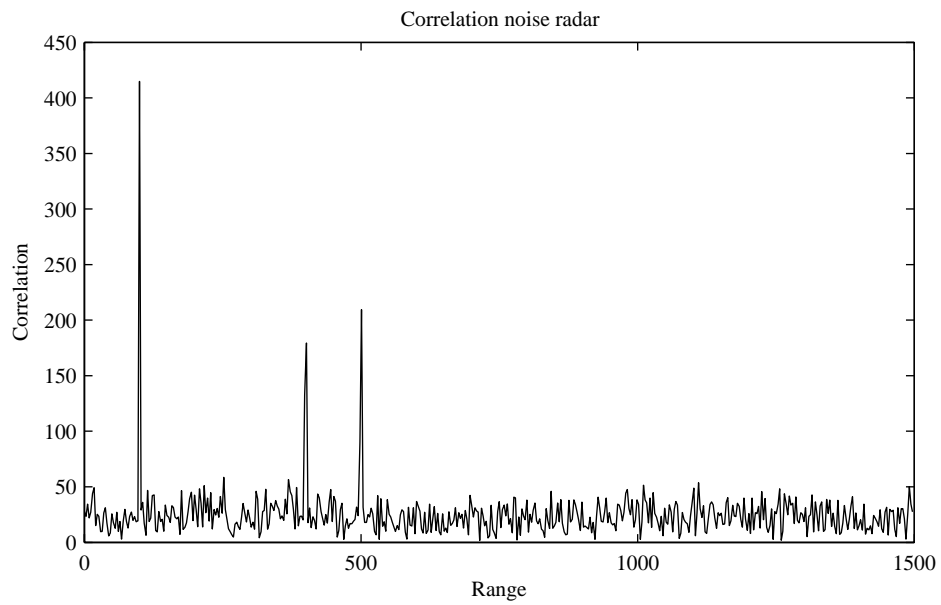


Figure 2: Correlation receiver example (three targets located at $r_1 = 100$ m, $r_2 = 400$ m and $r_3 = 500$ m).

2.2 Double Spectral Processing Receiver

The double spectral processing is another method of correlation measurements and another way of estimating the target's range [2]. In this case we first form the signal $s(t)$ as a sum of the received and transmitted signals

$$s(t) = x(t) + y(t) = x(t) + A_\sigma x(t - T_0) + \varepsilon(t). \quad (13)$$

The autocorrelation function of such a signal is:

$$\begin{aligned} R_{ss}(\tau) &= E[s(t)s^*(t - \tau)] \\ &= E[(x(t) + A_\sigma x(t - T_0) + \varepsilon(t)) \cdot (x^*(t - \tau) + A_\sigma^* x^*(t - \tau - T_0) + \varepsilon^*(t - \tau))] \\ &= R_{xx}(\tau) + A_\sigma^* R_{xx}(\tau + T_0) + R_{x\varepsilon}(\tau) + \\ &\quad + A_\sigma R_{xx}(\tau - T_0) + |A_\sigma|^2 R_{xx}(\tau) + A_\sigma R_{x\varepsilon}(\tau - T_0) + \\ &\quad + R_{\varepsilon x}(\tau) + R_{\varepsilon x}(\tau + T_0) + R_{\varepsilon\varepsilon}(\tau) \end{aligned} \quad (14)$$

Under the assumption that the noise $\varepsilon(t)$ is uncorrelated with the radar signal waveform $x(t)$ we get:

$$R_{ss}(\tau) = (1 + |A_\sigma|^2) R_{xx}(\tau) + A_\sigma^* R_{xx}(\tau + T_0) + A_\sigma R_{xx}(\tau - T_0) + R_{\varepsilon\varepsilon}(\tau) \quad (15)$$

The PSD of the signal $s(t)$ is of the form:

$$\begin{aligned} S_{ss}(\omega) &= FT_\tau[R_{ss}(\tau)] \\ &= S_{xx}(\omega)(1 + |A_\sigma|^2 + A_\sigma^* e^{j\omega T_0} + A_\sigma e^{-j\omega T_0}) + S_{\varepsilon\varepsilon}(\omega) \\ &= S_{xx}(\omega)|A_\sigma| \cos(\omega T_0 - \theta) + S_{xx}(\omega)(1 + |A_\sigma|^2) + S_{\varepsilon\varepsilon}(\omega) \end{aligned} \quad (16)$$

where θ is phase of A_σ . As we can see, the PSD of the analyzed signal can be divided into three parts. The first part is the modulated PSD of the transmitted signal while the second and third parts are the PSDs of the transmitted signal and noise, respectively. Let us assume that $S_{xx}(\omega) \approx \text{const.}$ and $S_{\varepsilon\varepsilon}(\omega) \approx \text{const.}$ In this case, the Fourier transform of the envelope of the PSD $S_{ss}(\omega)$ can be approximated as:

$$FT_\omega(|S_{ss}(\omega)|) \approx C_1 \delta(u - T_0) + C_1 \delta(u + T_0) + C_0 \delta(u) \quad (17)$$

where C_1 and C_0 are constants.

The delay T_0 can be estimated as the position of the maxima in the Fourier transform of the envelope of the signal's PSD.

In practical cases we have only one realization of the random process $s(t)$ and we can roughly estimate the PSD of the signal as the squared magnitude of the signal's Fourier transform

$$\hat{S}_{ss}(\omega) = |FT_t[s(t)]|^2 \quad (18)$$

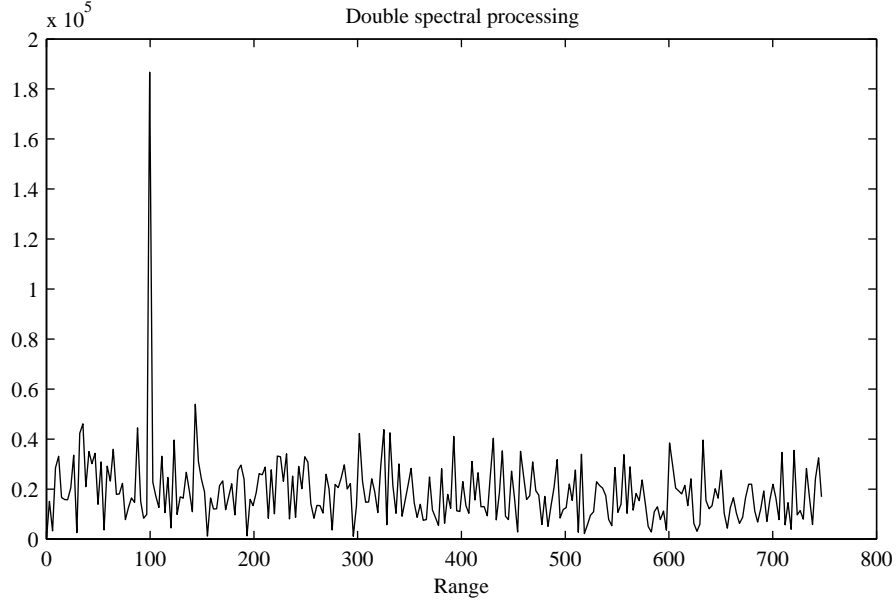


Figure 3: Double spectral processing receiver example (single target at $r_0 = 100$ m)

and by spectral processing of the obtained PSD estimate we get

$$P(u) = |FT_\omega[\hat{S}_{ss}(\omega)]| \quad (19)$$

The maximum value of $P(u)$ for $u > 0$ is located at $u = T_0$ and it can be used as an estimator of the target range since $r = \frac{1}{2}T_0c$.

2.2.1 Double Spectral Processing Receiver Simulation

In this simulation we use the radar carrier frequency $f_0 = 10$ GHz, bandwidth $B = 51.2$ MHz, and pulse repetition frequency PRF = 1000 kHz. The number of samples within the radar pulse is $N = BT_{int} = 512$. The range resolution is $\Delta r = \frac{c}{2B} = 2.93$ m. The target reflectivity is set to $A_\sigma = 1$. One target is simulated along the LOS at $r_1 = 100$ m. The double spectral processing is calculated according to the equation (19) and the results are presented in Figure 3. As expected, the sharp peak is found at $r = 100$ m. Note that the u axis is appropriately scaled to represent the real range coordinate.

2.3 Mutual Interference

When two or more radar systems operate in proximity at the same frequency band, they could produce a scenario where mutual interference (MI) is experienced.

In the presented model, we assume that there are N_R continuous radars with random waveforms operating simultaneously at the same frequency band. We will consider the simplest scenario of a single-point target. Each radar transmits a signal $x_i(t)$ where $i = 1, 2, \dots, N_R$. At the receiver of the k -th radar, the received signal is of the form:

$$y_k(t) = K_{1,k}x_1(t - t_{d,1,k}) + K_{2,k}x_2(t - t_{d,2,k}) + \dots + K_{k,k}x_k(t - t_{d,k,k}) + \dots + K_{N_R,k}x_{N_R}(t - t_{d,N_R,k}) + \varepsilon(t) \quad (20)$$

Time delays $t_{d,i,k}$ are proportional to the total distance $r_{i,k}$, i.e. from i -th radar to target and then from target to k -th radar. Amplitude coefficients $K_{i,k}$ are proportional to the target reflectivity and to $r_{i,k}^{-2}$. $\varepsilon(t)$ is noise at the receiver side. It is obvious that components like $K_{k,k}x_k(t - t_{d,k,k})$ of the received signal $y_k(t)$ are of interest where all other components represent interference.

Since all radars use a noise waveform, we can calculate the equivalent noise at the receiver and model the received signal as:

$$y_k(t) = K_{k,k}x_k(t - t_{d,k,k}) + \varepsilon_{eq}(t) \quad (21)$$

where the power of the equivalent noise $\varepsilon_{eq}(t)$ is equal to the sum of the powers of each interference return and the power of noise $\varepsilon(t)$. The returned signal is processed by the correlation receiver as described in Section 2.1.

2.3.1 Mutual Interference Simulation

In this simulation three noise radars are considered. The target and radar positions are shown in Figure 4. The first and second radars are located at the same position, while the third radar is shifted. All three radars operate at the same frequency of 10 GHz with a 25 MHz bandwidth. The PRF for the first and third radars is 97.7 kHz and the PRF for the second radar is 116 kHz. Note that the first and third radars have the same parameters whereas the second radar differs slightly. The radar parameters are given in Table 1. It is assumed that the target moves with constant velocity 200 m/s along the first and second radars' LOS. Equations (21) and (11) are used to perform the calculations in this simulation.

Five cases with respect to the three radars' output powers are considered:

1. The three radars operate with the same power. Range Doppler profiles are shown in Figure 5. The upper row shows the radar returns of the first , second

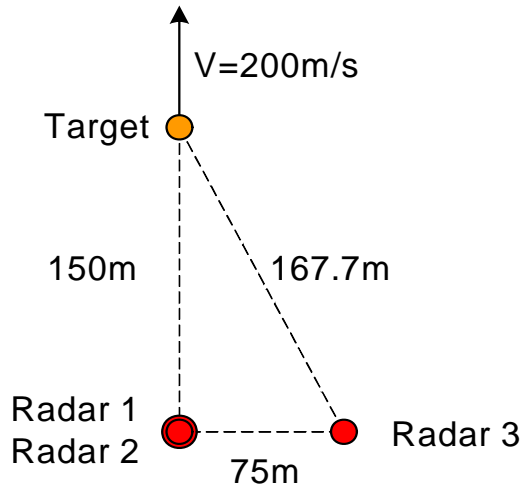


Figure 4: Location of three radars

- and third radars without MI (only one radar is active) while the lower row shows the radar returns of the first, second and third radars with MI (all three radars are active). In this scenario, the influence of one radar on the others is negligible.
2. The first radar's power is 20 dB higher than the third radar's power, while the second radar's power is 3 dB higher than the third one. Results are shown in Figure 6. The upper row shows the radar returns of the first, second and third radars without MI (only one radar is active) while the lower row shows the radar returns of the first, second and third radars with MI (all three radars are active).
 3. The first radar's power is 30 dB higher than the third radar's power, while the second radar's power is 3 dB higher than the third one. Results are shown in Figure 7. The upper row shows the radar returns of the first, second and third radars without MI (only one radar is active) while the lower row shows the radar returns of the first, second and third radars with MI (all three radars are active).
 4. The first radar's power is 35 dB higher than the third radar's power, while the second radar's power is 3 dB higher than the third one. Results are shown in Figure 8. The upper row shows the radar returns of the first, second and third radars without MI (only one radar is active) while the lower row shows the radar returns of the first, second and third radars with MI (all three radars are active). Note that the third radar is not able to detect the target.
 5. The first radar's power is 40 dB higher than the third radar's power, while the

Table 1: Radar parameters

Radar Number	1	2	3
Operating frequency	10 GHz	10 GHz	10 GHz
Bandwidth	25 MHz	25 MHz	25 MHz
Pulse repetition frequency	97.7 kHz	119 kHz	97.7 kHz
Coherent integration time	2.62 ms	2.56 ms	2.62 ms

second radar’s power is 3 dB higher than the third one. Results are presented in Figure 9. The upper row shows the radar returns of the first, second and third radars without MI (only one radar is active) while the lower row shows the radar returns of the first, second and third radars with MI (all three radars are active). The third radar is not able to detect the target.

Figures 5-9 show that in all cases, the first and second radars successfully detect the target’s range and velocity. In cases 4 and 5, the third radar is not able to detect either of the target’s parameters because of the influence from radar 1 and radar 2 on radar 3. Another observation is that there is no significant influence from radar 2 and radar 3 on radar 1 since radar 1 has the highest transmit power. Radar 1 introduces noise in the range-Doppler profiles of the radar 2 and radar 3. These results suggest that the noise radar can operate with low SNR (up to -30 dB). However when the interference signal is 40 dB or above, the radar is not able to detect target. The interference does not introduce “ghost targets”. This study indicates that for noise radars the signal transmitted from one radar is treated as noise for other radars, which suggests that more than one radar can share the same bandwidth. They will effectively raise the overall noise floor though.

2.3.2 Comparison Between noise radar and Conventional LFM Radar

In this section we evaluate the mutual interference effects on noise radars and linear frequency modulated (LFM) waveform radars from other such radars when determining the range and velocity of the moving target. Let us consider three X-band radars, each operating at a center frequency of 10 GHz with 150 MHz bandwidth. Assume a single-point target located at (0 m, 0 m, 100 m) with velocity $V_{tg} = 100 \frac{m}{s}$. Radar locations are (3010 m, 0 m, 0 m) for the first radar, (3080 m, 0 m, 0 m) for the second radar, and (2000 m, -2300 m, 0 m) for the third radar. The first and third radars have the same transmit power while the transmit power of the second radar is 16 times (12 dB) higher. The target to radar distance is 3011.7 m for the first radar, 3081.6 m for the second radar and 3049.6 m for the third radar. The projection of the target’s

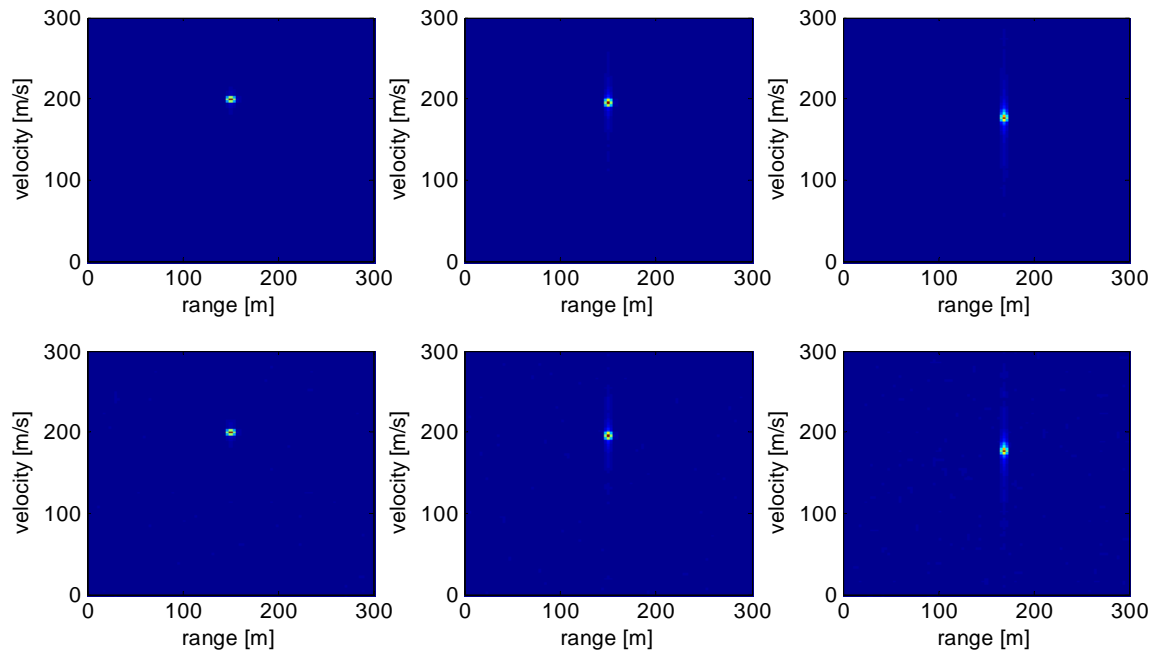


Figure 5: Range-Doppler profiles. Radars operate with the same transmit power. Upper row: radar returns of the first, second and third radars without MI. Lower row: radar returns of the first, second and third radars with MI.

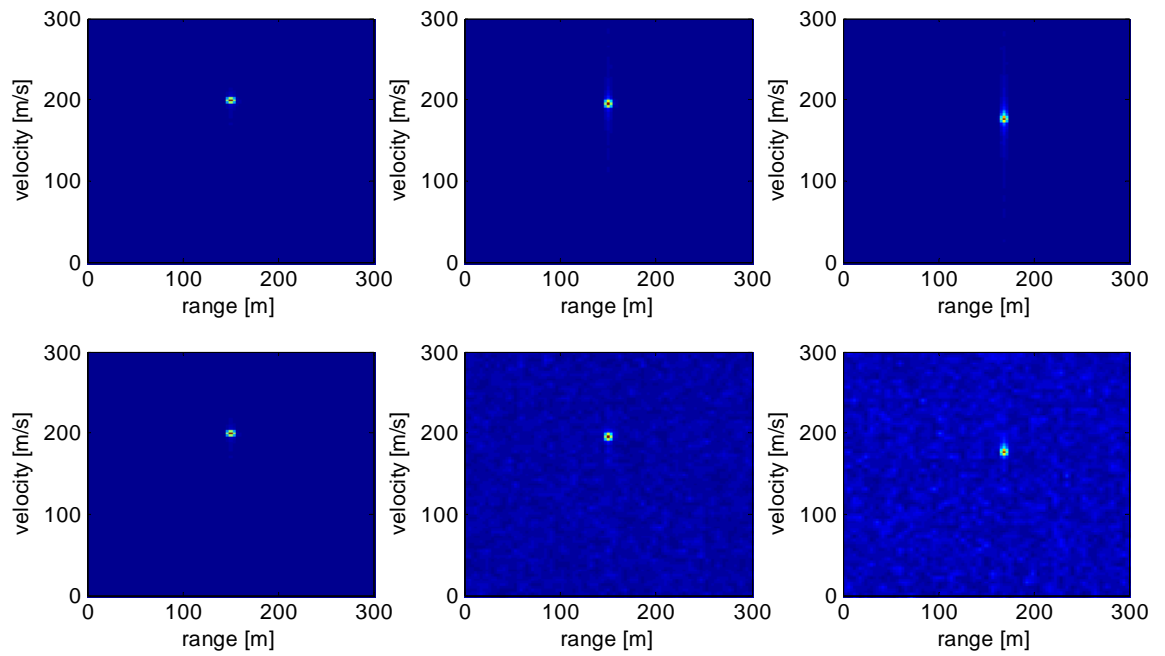


Figure 6: Range-Doppler profiles. Radars operate with the following relative transmit powers: +20 dB, +3 dB and 0 dB. Upper row: radar returns of the first, second and third radars without MI. Lower row: radar returns of the first, second and third radars with MI.

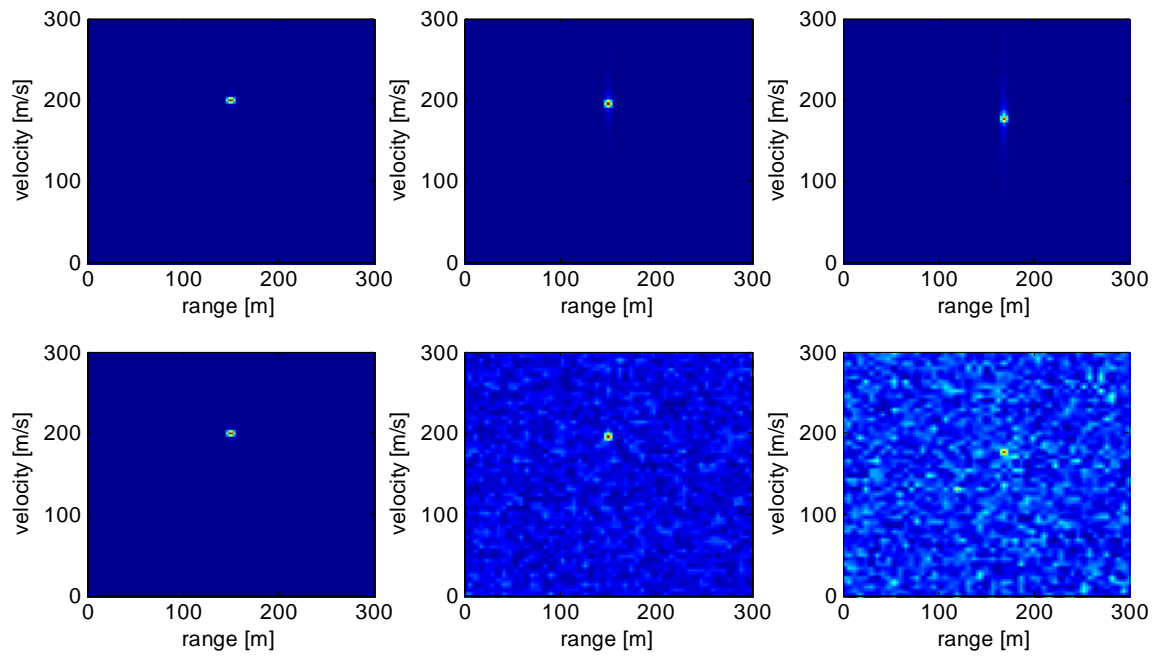


Figure 7: Range-Doppler profiles. Radars operate with the following relative transmit powers: +30 dB, +3 dB and 0 dB. Upper row: radar returns of the first, second and third radars without MI. Lower row: radar returns of the first, second and third radars with MI.

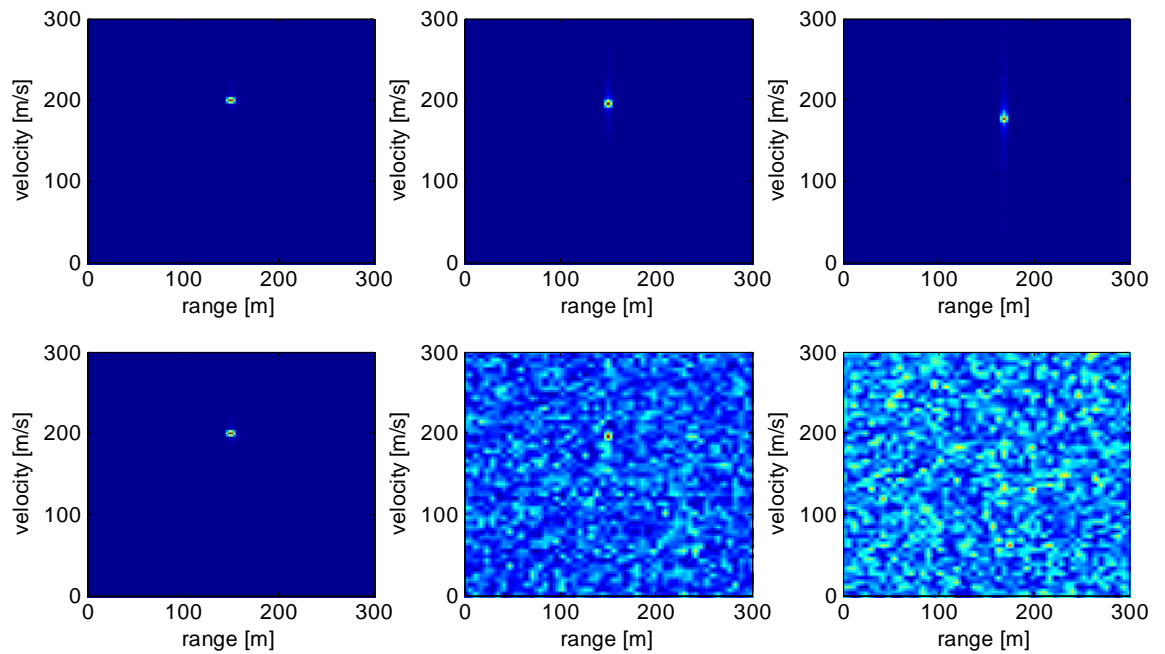


Figure 8: Range-Doppler profiles. Radars operate with the following relative transmit powers: +35 dB, +3 dB and 0 dB. Upper row: radar returns of the first, second and third radars without MI. Lower row: radar returns of the first, second and third radars with MI.

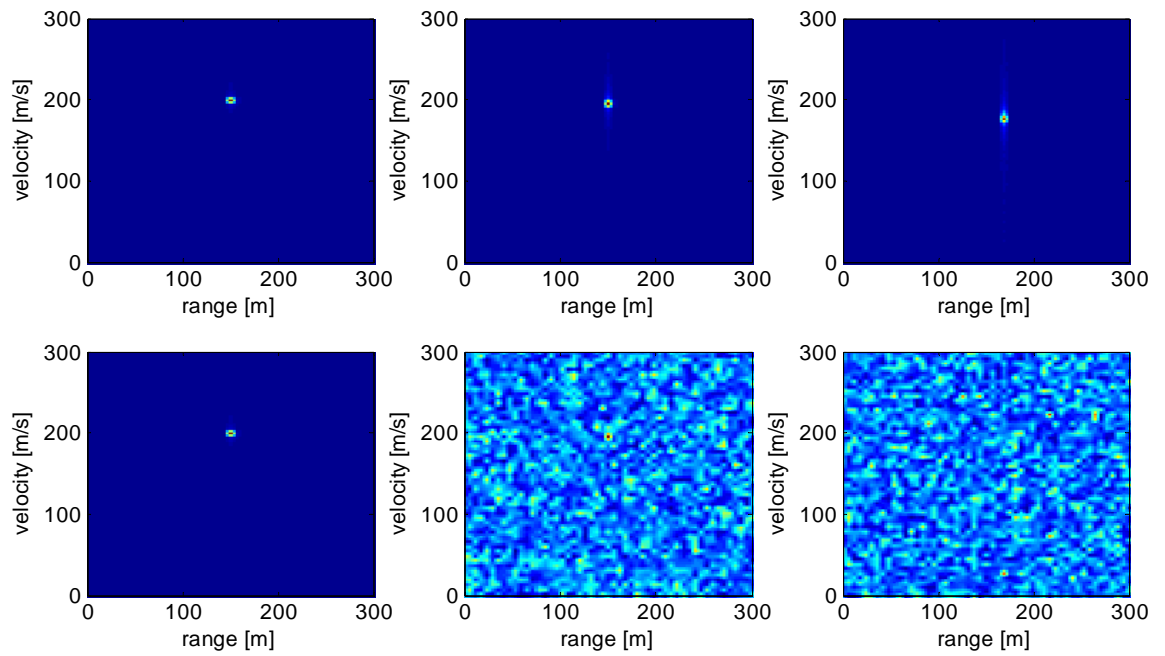


Figure 9: Range-Doppler profiles. Radars operate with the following relative transmit powers: +40 dB, +3 dB and 0 dB. Upper row: radar returns of the first, second and third radars without MI. Lower row: radar returns of the first, second and third radars with MI.

velocity onto the radar LOS is $99.94 \frac{\text{m}}{\text{s}}$ for the first radar, $99.95 \frac{\text{m}}{\text{s}}$ for the second radar and $-65.58 \frac{\text{m}}{\text{s}}$ for the third radar. The radars transmit a series of 128 pulses and the total integration time is 3.5 ms. The number of samples within one pulse is 4096. Equations (21) and (11) are used to perform the calculations in this simulation.

Two cases are considered:

1. The radars' waveforms are LFM signals.
2. The radars use a random noise waveform.

The results are presented in Figure 10 for the first case and Figure 11 for the second case. The figures consist of 6 subplots where each row corresponds to one radar. The left column plots present range-Doppler profiles for the case when only one radar is operating, while the right column plots present range-Doppler profiles for the case when all three radars are operating simultaneously. The simulation model assumes that the radars operate coherently.

In the conventional LFM case, only the second radar (highest power) gives a satisfactory range-Doppler profile when all radars are operating simultaneously. The first and third radar profiles result in targets with the wrong range and velocity (ghost targets).

In the noise waveform case, each radar detects true target parameters in solo and simultaneous operation modes. The influence of the second radar on the remaining two is expressed through a higher noise level at the receiver (first and third row, right subplots in Fig.11).

Figures 12 and 13 present the same setup with equal radar transmit powers. Ghost targets in the case of LFM radars have become points with equal (very close) magnitude, while interference in the case of noise radars is lower than in the previous case. In all cases, the true target position in the range-Doppler domain is marked with a red circle.

This study suggests that noise radars can operate in the same frequency band. The mutual interference involves at higher level of noise only, and can decrease the maximum detection range of the target. On the other hand, LFM radars can produce "ghost" targets when more than one radar operate in same frequency band. The results show that noise radars are unlikely to interfere with other noise radar systems or other radar systems in the same band.

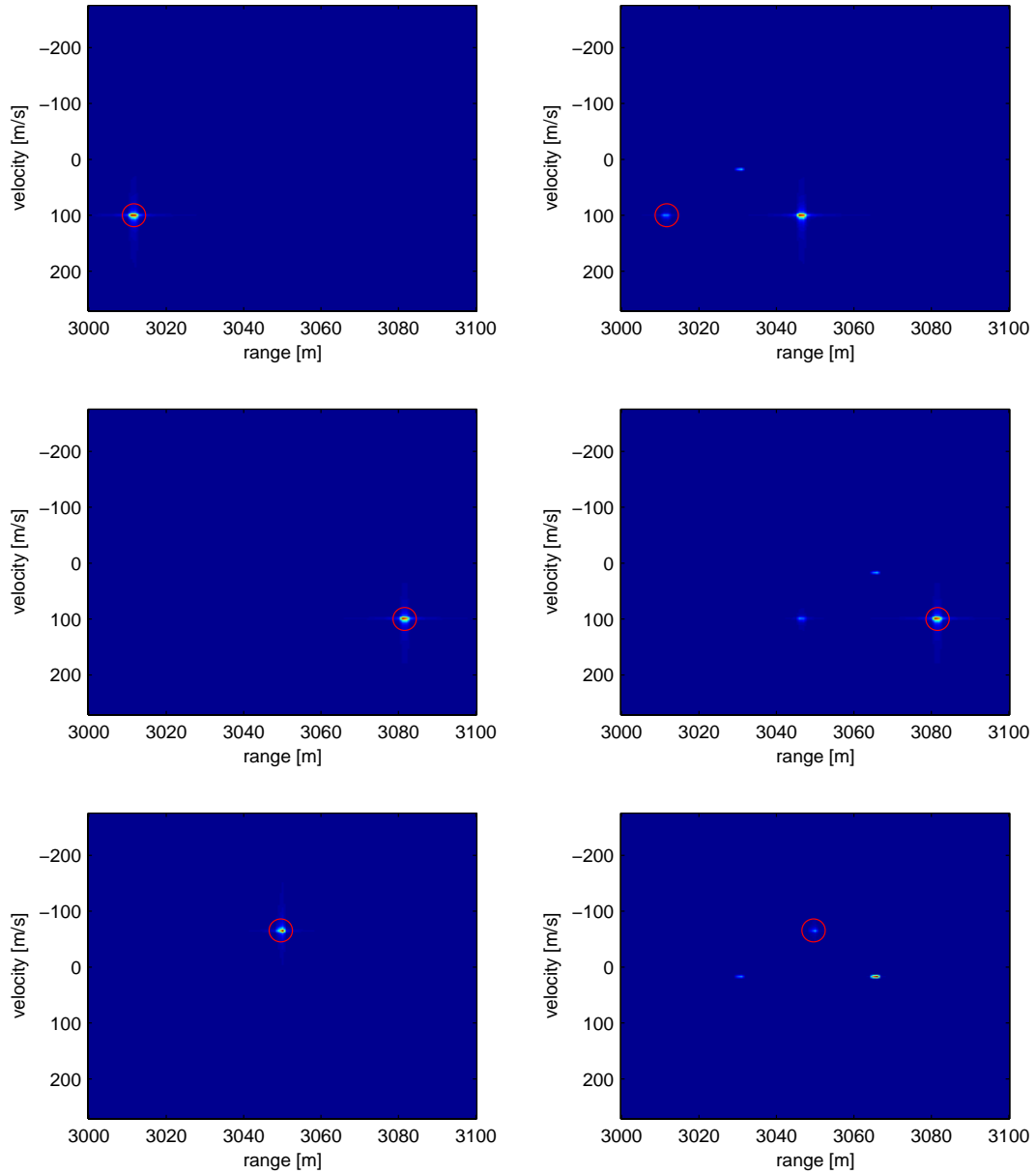


Figure 10: Conventional LFM radars. Three radars are considered. Subplots on the left side present range-Doppler profiles when the radars operate without interference. Subplots on the right side show interference effects when the radars operate simultaneously. The second radar's transmit power is 12 dB higher than the transmit powers of the first and third radars.

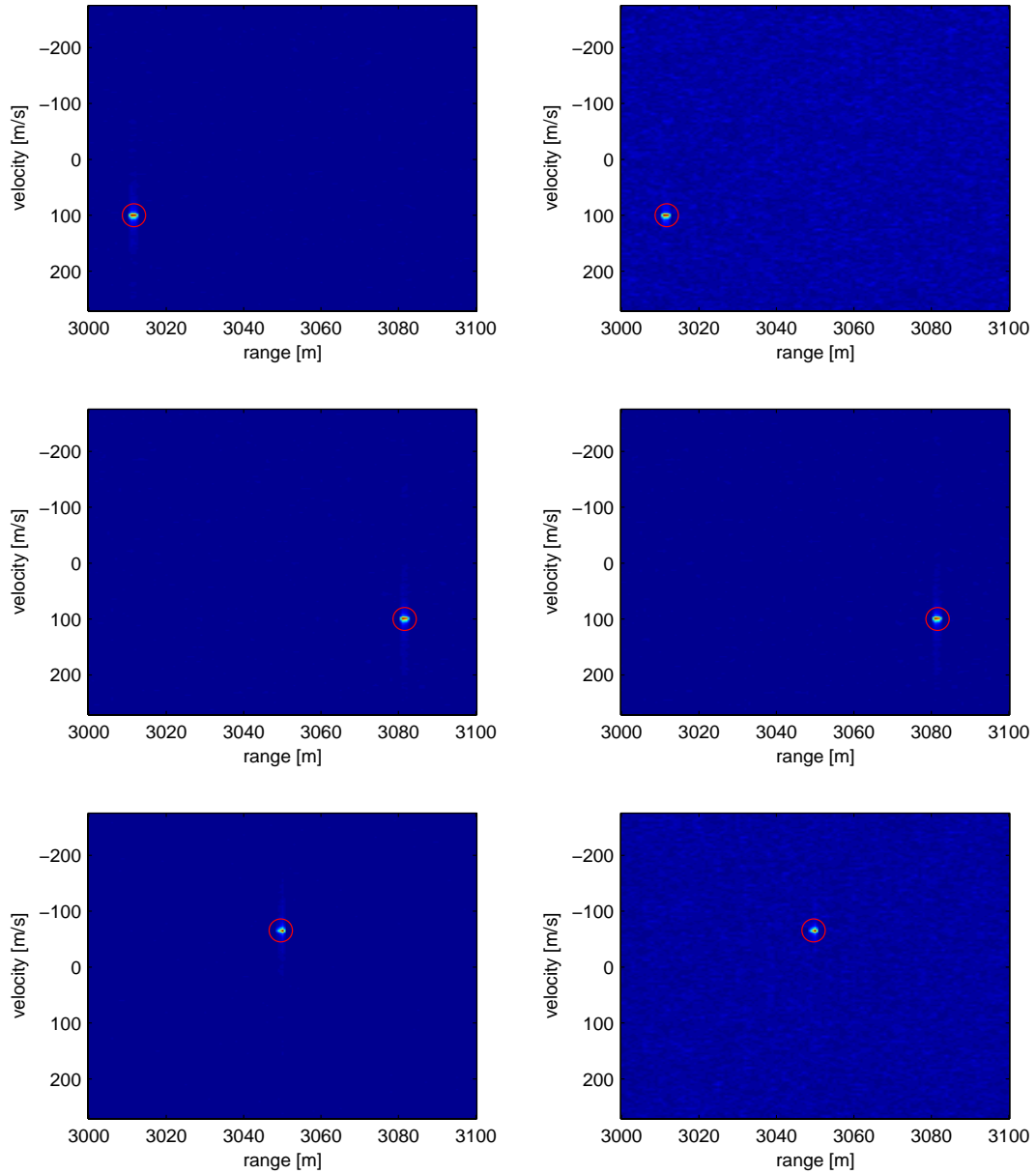


Figure 11: Random waveform radars. Three radars are considered. Subplots on the left side present range-Doppler profiles when the radars operate without interference. Subplots on the right side show interference effects when the radars operate simultaneously. The second radar's transmit power is 12 dB higher than the transmit power of the first and third radars.

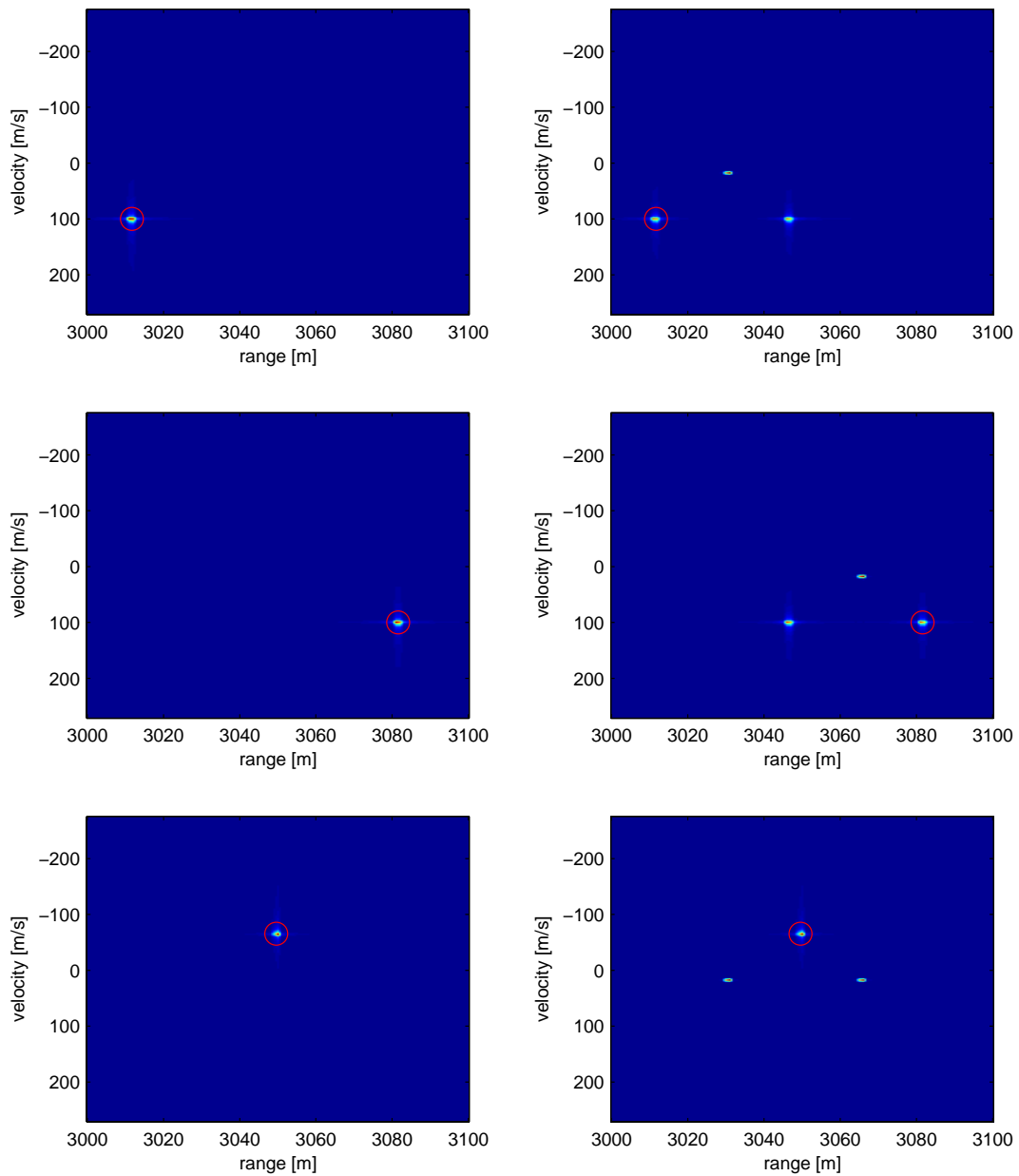


Figure 12: Conventional LFM radars. Three radars are considered. Subplots on the left side present range-Doppler profiles when the radars operate without interference. Subplots on the right side show interference effects when the radars operate simultaneously. All radars operate with same transmit power.

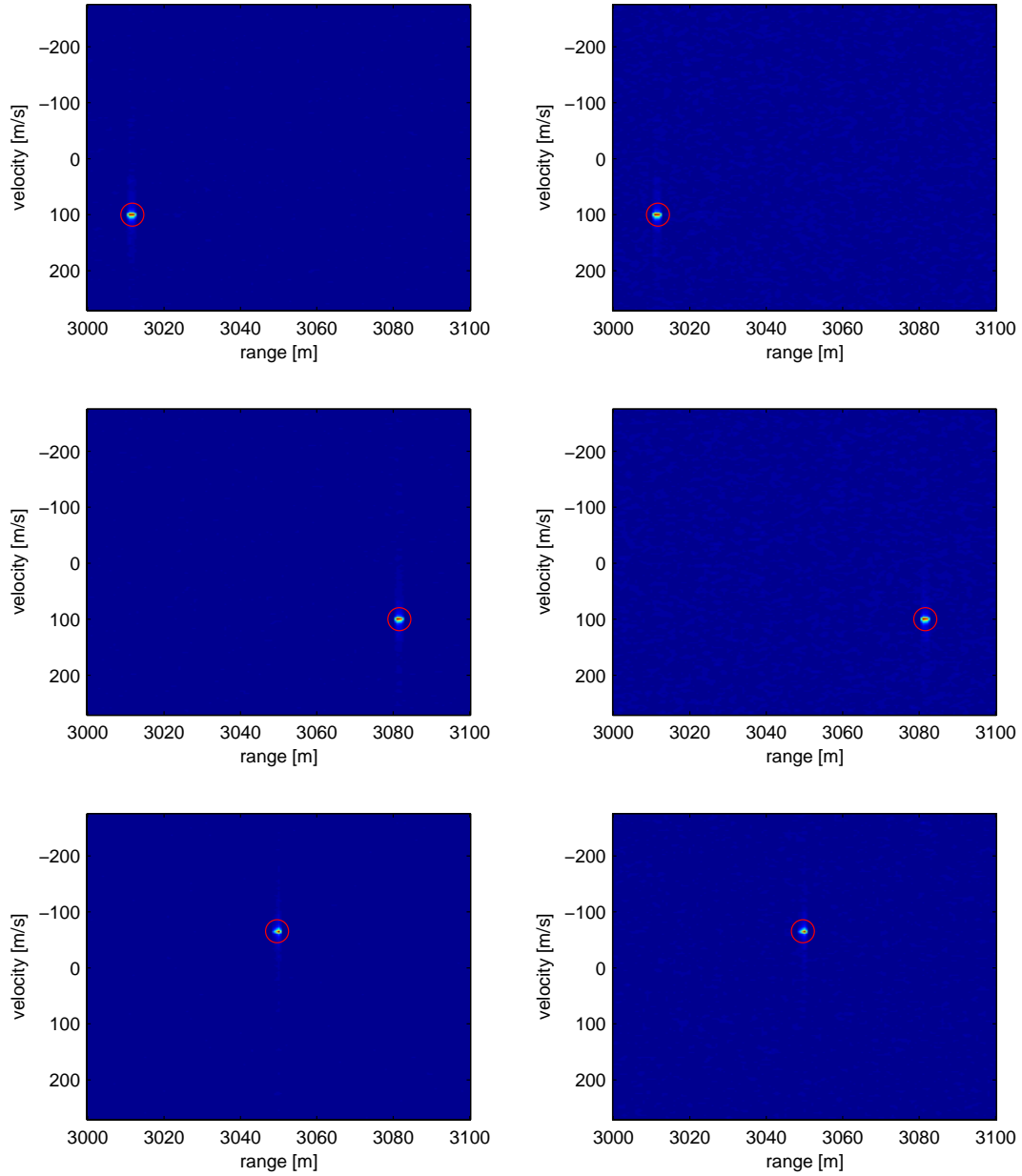


Figure 13: Random waveform radars. Three radars are considered. Subplots on the left side present range-Doppler profiles when the radars operate without interference. Subplots on the right side show interference effects when the radars operate simultaneously. All three radars operate with the same transmit power.

2.4 Probability of Interception

Radars with conventional LFM waveforms transmit a series of identical pulses, so the easiest way to detect these radar signals is through observation over a long period of time and then examination of the Fourier spectrum of the observed signal. The decision as to whether the radar signal is present in the noise or not can be derived by comparison of the maximum value in the Fourier spectrum with some threshold level, where the threshold level should be dependent on noise. With increasing observation time, the maximum value of the Fourier spectrum can be increased within the considered frequency range significantly.

On the other hand, noise radars use stochastic waveforms and they are not periodic. The observed signal does not exploit periodicity for long observation times and the Fourier spectrum is equally distributed over the whole frequency band. That implies low probability of interception. This heuristic analysis is presented in Figure 14 for 10 dB SNR, Figure 15 for 0 dB SNR and Figure 16 for -6 dB SNR. In this simulation, the Fourier spectrum of the observed signal in the case of a conventional LFM radar and a noise radar for various observation times are studied; $N_p=2,4,8,16$, and 32 radar pulses are used. There are 64 samples in each pulse. Figures 14-16 suggest that the conventional radar exhibits better detection compared with the noise radar in the same noisy environment. The obvious reason is that the deterministic waveform such as LFM involves periodicity. The periodic pulses can be detected by Fourier transform (spectrum analyzer). However stochastic waveforms are not periodic and therefore are not easy to detect by spectral analysis. The probability of interception increases rapidly when observation time increases in case of conventional LFM radar. However the probability of interception does not depend significantly on observation time in the case of random waveform radar.

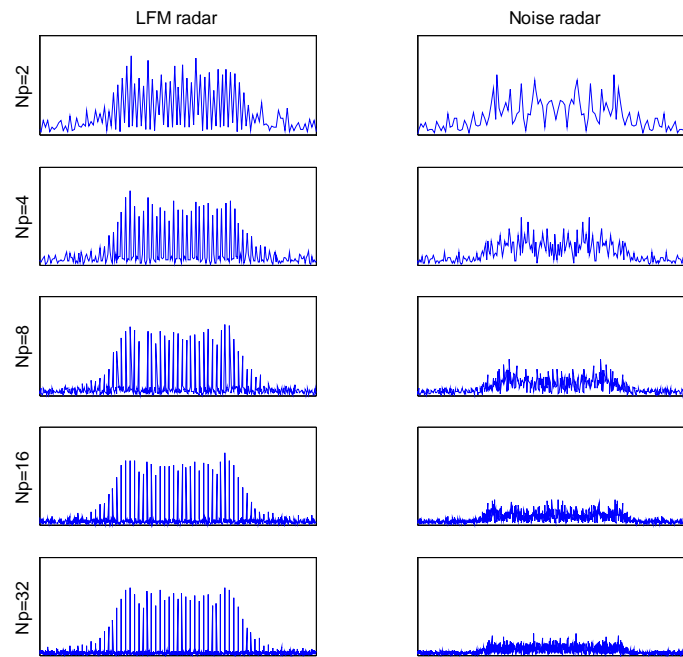


Figure 14: Fourier spectrum of the observed signal in the case of a conventional LFM radar (left) and a NR (right) for various observation times. N_p is the number of radar pulses within the observation time. The signal to noise ratio is 10 dB.

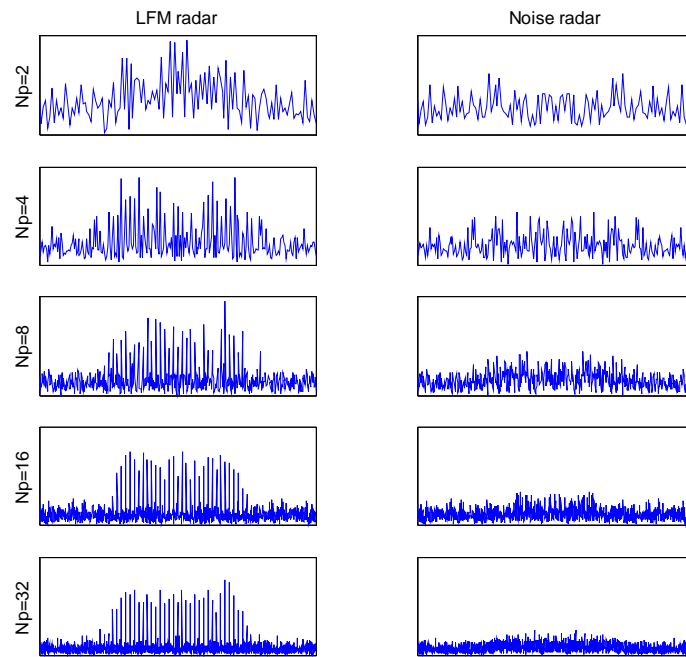


Figure 15: Fourier spectrum of the observed signal in the case of a conventional LFM radar (left) and a NR (right) for various observation times. N_p is the number of radar pulses within the observation time. The signal to noise ratio is 0 dB.

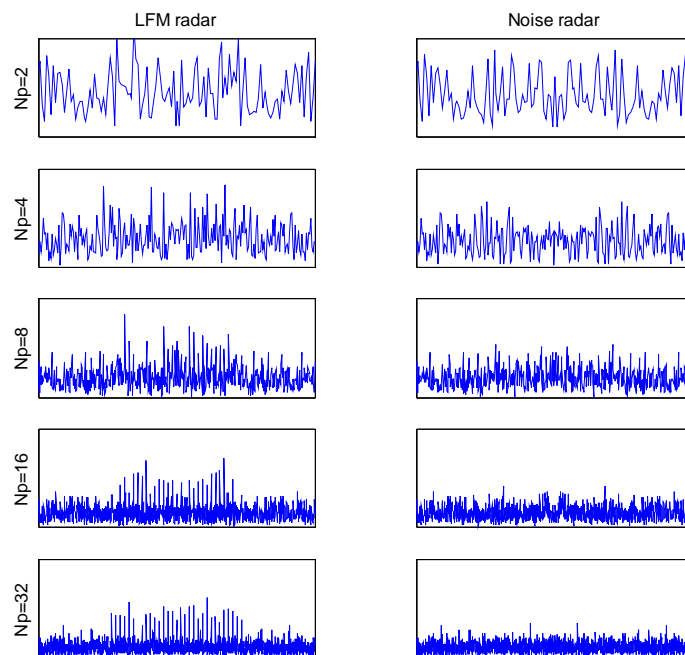


Figure 16: Fourier spectrum of the observed signal in the case of a conventional LFM radar (left) and a NR (right) for various observation times. N_p is the number of radar pulses within the observation time. The signal to noise ratio is -6 dB.

3 Discussion and Conclusion

This report presents an overview of the basic principles of noise radar technology (NRT). NRT is not currently in wide use. Only recently have achievements necessary to NRT's implementation have become available. The rapid advancement of digital signal processing algorithms, signal processing hardware, new methods for generation of noise waveforms, solid state microwave techniques, and integrated circuit electronics, the realization of noise radar is relatively easy.

This report provides theoretical evaluations and simulation evaluations of NRT that support its use in current and future applications. We evaluated two methods of coherent processing of noise waveform returns, the correlation and double spectral processing receivers. Both methods combine the transmitted and received noise waveforms in such a way that the range of the target can be determined. Simulation results show that both methods determine the unambiguous range of the target. We evaluated the mutual interference effects on noise radars and linear frequency modulated (LFM) waveform radars from other radars when determining the range and velocity of the moving target. The results show that noise radars are unlikely to interfere with other noise radar systems or other radar systems in the same band. An evaluation of the probability that the noise radar's noise waveform is intercepted is also studied. It is shown that in a variety of noisy environments, the noise radar always has a much lower LPI than the conventional LFM radar. The noise radar's exceptional performance in the above evaluations indicates that it is a suitable radar system for a variety of applications. The following three potential applications are identified for the future research at DRDC. It should be noted that the through-wall sensing is an ongoing research at the DRDC.

3.1 Through wall surveillance

Recent terrorist activities and law-enforcement situations involving hostage situations underscore the need for effective through-wall detection. Through wall imaging technology has been developed for many years. However, there are still many improvements that can be implemented in next generation radar systems, especially with regard to covertness of the transmit signal and immunity from interference and jamming. Current building interior imaging systems are based on short-pulse waveforms, which require specially designed antennas to subdue unwanted ringing. In addition, periodically transmitted pulses of energy are easily recognizable by the intelligent adversary who may employ appropriate countermeasures to confound detection. A polarimetric UWB noise has a great promise in its ability to covertly detect obscured targets [25]. The main advantages of the random noise radar lie in two aspects: first, random noise waveform has an ideal "thumbtack" ambiguity function, i.e., its down range and cross range resolution can be separately controlled, thus providing unam-

ambiguous high resolution imaging at any distance; second, random noise waveform is inherently low probability of intercept (LPI) and low probability of detection (LPD), i.e., it is immune from detection, jamming, and interference. Thus, it is an ideal candidate sensor for covert imaging of obscured regions in hostile environments.

3.2 Random noise polarimetry for high-resolution subsurface probing applications

One of the potential applications is a random noise polarimetry for high-resolution subsurface probing applications [15], which can deliver to the war-fighter superior knowledge of the battle-space in difficult environments (intentional and non-intentional environments) such as in Afghanistan and Iraq. Ground-penetrating or subsurface radar systems are increasingly being used for a variety of military applications and operations in Afghanistan and Iraq. Although such systems are essentially similar to other free-space radar systems, they present certain unique problems that demand specialized system design and signal processing capabilities. Some of the primary issues that need special attention are efficient coupling of the electromagnetic energy into the ground, elimination of the large reflection from the air-to-ground interface, achieving adequate penetration into sometimes lossy media, and achieving adequate signal bandwidth consistent with desired depth resolution. From a phenomenological point of view, factors such as propagation loss, clutter characteristics, and target characteristics are quite different from free-space systems. Ground-penetrating radar systems operate over a wide range of probing depths, from close-range high-range applications such as locating buried mines and hidden voids in pavements at depth of up to 50 cm, to long-range low-resolution applications such as probing geologic strata at depths of over 100 m. Most of the ground-penetrating radars use either linear frequency modulation (LFM) or step-frequency waveforms. However the random noise polarimetry has its unique merits. This unique concept synergistically combines the advantages of a random noise ultra-wideband waveform with the power of coherent processing to provide a powerful technique for obtaining high-resolution images.

3.3 Random noise polarimetry for high-resolution foliage penetration applications

Among other SAR/ISAR applications, one of the potential applications is a foliage penetration (FOPEN) polarimetric SAR imaging using random noise waveforms [21], which can deliver to the war-fighter superior knowledge under difficult conditions and environments that may include high target density, low-observable manoeuvring threats, heavy clutter and jamming such as in Afghanistan and Iraq. As is known,

when using a SAR to image targets under dense foliage, the foliage obscures the target images in three major ways. 1) The foliage attenuates the energy both incident to and scattered from the target, resulting in a lower signal-to-noise ratio. 2) The foliage forms strong backscatter clutter, reducing the target-to-background contrast in the image. 3) The amplitude and phase fluctuation of the foliage distorts the SAR images of the target. The first and second issues relate to the mean attenuation and the backscatter, respectively, while the third relates to the amplitude and phase fluctuations of the foliage. The detection and identification of targets obscured by foliage have been topics of great current interest for the military. Several SAR experiments have demonstrated promising images of terrain and man-made objects obscured by dense foliage, by either using linear frequency modulation (LFM) or step-frequency waveforms. The random noise waveform has its special merits. Because of the randomness and wide bandwidth of the transmit waveform, such a radar has the potential for covert detection and identification, and is relatively immune from hostile detection and jamming while preserving very high resolution. In addition NRT provides excellent potential capabilities for unambiguous and simultaneous range and Doppler measurements with high resolution and accuracy as a result of the non-periodic waveform. Furthermore, there is no theoretical limitation in the unambiguous working range of NRT.

References

- [1] Xu, X. (2003). Impact of Different Correlation Receiving Techniques on the Imaging Performance of UWB Random Noise, *Geoscience & Remote Sensing Symposium*, IGARSS'03, Vol. 7, pp. 4,525-4,527.
- [2] Lukin, K. A. (2002). Developments of Noise Radar Technology in LNDES IRE NASU, First International Workshop on the Noise Radar Technology, *NTRW 2002 Proceedings*, pp. 90-96, Yalta, Ukraine.
- [3] Axelsson, S. R. J. (2000). On the Theory of Noise Doppler Radar, *Geoscience and Remote Sensing Symposium Proceedings 2000*, pp. 856-860, Honolulu, USA.
- [4] Axelsson, S. R. J. (2003). Noise Radar For Range/Doppler Processing and Digital Beamforming Using Low-Bit ADC, *IEEE Trans. on Geoscience and Remote Sensing*, Vol. 41, No. 12, pp. 2,703-2,720.
- [5] Horton, B. M. (1959). Noise-Modulated Distance Measuring Systems, *Proceedings of the IRE*, Vol. 47, pp. 821-828.
- [6] Lukin, K. A. (2002). The Principles of Noise Radar Technology, First International Workshop on the Noise Radar Technology, *NTRW'2002 Proceedings*, pp. 13-22, Yalta, Ukraine.
- [7] Bell, D. C. and Naryanan, R. M. (2001). Theoretical Aspects of Radar Imaging Using Stochastic Waveforms, *IEEE Trans. on Signal Processing*, Vol. 49, No. 2, pp. 394-400.
- [8] Stephan, R. and Loele, H. (2000). Theoretical and Practical Characterization of a Broadband Random Noise Radar, *Dig. 2000 IEEE MTT-S International Microwave Symp.*, pp. 1,555-1,558, Boston, MA.
- [9] Guosui, L., Hong, G., and Weimin, S. (1999). Development of Random Signal Radars", *IEEE Trans. on Aerospace and Electronic Systems*, Vol. 35, No. 3, pp. 770-777.
- [10] Kalinin, V. I., Lyubchenko, V. E., and Panas, A. I. (2005). Wideband wireless communication with spectral processing of noise continuous waveform, *Proceedings XXVIIIth General Assembly of International Radio Science Union URSI-GA*, CD-ROM, New Delhi, India.
- [11] Liu, G. and Gu, H. (1997). The present and the future of random signal radars, *IEEE Aerospace and Electronics Systems Magazine*, Vol. 12, No. 10, pp. 35-40.

- [12] Liu, G., Gu, H., and Su, W. (1999). The development of random signal radar. *IEEE Transaction on Aerospace and Electronic Systems*, Vol. 35, No. 3, pp. 770-777.
- [13] Cooper G. R. and McGillem, C. D. (1967). Random signal radar, Purdue Univ., West Lafayette, IN, Final Report.
- [14] Guosui, L., Xiangquan, S., Jinhui, L., Guoyu, Y., and Yaoliang, S. (1991). Design of noise FW-CW radar and its implementation, *Proc. Inst. Elect. Eng. Radar Signal Process.*, Vol. 138, No. 5, pp. 420-426.
- [15] Narayanan, R. M., Xu, Y., Hoffmeyer, P. D., and Curtis, J. O. (1998). Design, performance, and implementation of a coherent ultrawideband random noise radar, *Opt. Eng.*, Vol. 37, No. 6, pp. 1,855-1,869.
- [16] Lukin, K. A. (1998). Millimeter wave noise radar technology, *Proc. 3rd Int. Kharkov Symp., Physics Engineering millimeter and Submillimeter Waves*, Kharkov, Ukraine, pp. 94-97.
- [17] Theron, I. P., Walton, E. K., Gunawan, S., and Cai, L. (1999). Ultrawide-band noise radar in the VHF/UHF band, *IEEE Trans. Antennas Propagat.*, Vol. 47, pp. 1,080-1,084.
- [18] Theron, I. P., Walton, E. K., and Gunawan, S. (1998). Compact range radar cross-section measurements using a noise radar, *IEEE Trans. Antennas Propagat.*, Vol. 46, pp. 1,285-1,288.
- [19] Garmatyuk, D. S. and Narayanan, R. M. (2002). Ultra-wideband continuouswave random noise arc-SAR, *IEEE Trans. Geosci. Remote Sensing*, Vol. 40, pp. 2,543-2,552.
- [20] Narayanan, R. M. and Dawood, M. (2000). Doppler estimation using a coherent ultra wide-band random noise radar, *IEEE Trans. Antennas Propagat.*, Vol. 48, pp. 868-878.
- [21] Xu, X. and Narayanan, R. M. (2001). FOPEN SAR imaging UWB step-frequency and random noise waveforms, *IEEE Trans. Aerosp. Electron. Syst.*, Vol. 37, pp. 1,287-1,300.
- [22] Xu, X. and Narayanan, R. M. (2001). Three-dimensional interferometric ISAR imaging for target scattering diagnosis and modeling, *IEEE Trans. Image Processing*, Vol. 10, pp. 1,094-1,102.
- [23] Xu, Y., Narayanan, R. M., Xu, X., and Curtis, J. O. (2001). Polarimetric processing of coherent random noise radar data for buried object detection, *IEEE Trans. Geosci. Remote Sensing*, Vol. 39, pp. 467-478.

- [24] Xu, X. and Narayanan, R. M. (2001). Range sidelobe suppression technique for coherent ultra-wideband random noise radar imaging, *IEEE Trans. Antennas Propagat.*, Vol. 49, pp. 1,836-1,842.
- [25] Lai, C. P., Narayanan, R. M. Colkowski, G. (2006). Through wall surveillance usig ultrawideband random noise radar, *25 th Army Science Conference*, Florida, November 27-30, Orlando, Florida, pp. 1-4.

Distribution list ■

DRDC Ottawa TM 2006-266

Internal distribution ■

- 1 Thayananthan Thayaparan
- 1 Christopher Wernik
- 1 Gary Geling
- 1 David Schlingmeier
- 1 Paris Vachon
- 1 Doreen Dyck
- 1 Brian Eatock
- 1 Jeff Secker
- 1 Chen Liu
- 1 Karim Mattar
- 1 Ramin Sabry
- 1 David DiFilippo
- 1 Edwin Riseborough
- 1 Silvester Wong
- 1 Greg Barrie
- 1 Ryan English
- 3 Library

Total internal copies: 19

External distribution ■

Department of National Defence

- 1 ADM(ST) (for distribution)
- 1 DRDKIM 3
- 1 J2 STI
- 1 DGOR (Library)
- 1 DSTL 2
- 1 DSTL
- 1 DSTA
- 1 DSTM
- 1 DSTCCIS 5
- 1 D Space D 2
- 1 J2 GICI
- 1 CFJIC (D Squadron)
- 1 CISTI
- 2 Library and Archives Canada

Total external copies: 15

Total copies: 34

DOCUMENT CONTROL DATA		
(Security classification of title, body of abstract and indexing annotation must be entered when document is classified)		
1. ORIGINATOR (the name and address of the organization preparing the document. Organizations for whom the document was prepared, e.g. Centre sponsoring a contractor's report, or tasking agency, are entered in section 8.) Defence R&D Canada – Ottawa 3701 Carling Avenue, Ottawa, Ontario, Canada K1A 0Z4	2. SECURITY CLASSIFICATION (overall security classification of the document including special warning terms if applicable). UNCLASSIFIED	
3. TITLE (the complete document title as indicated on the title page. Its classification should be indicated by the appropriate abbreviation (S,C,R or U) in parentheses after the title). Noise Radar Technology Basics		
4. AUTHORS (last name, first name, middle initial) Thayaparan, T.; Wernik, C.		
5. DATE OF PUBLICATION (month and year of publication of document) December 2006	6a. NO. OF PAGES (total containing information. Include Annexes, Appendices, etc). 46	6b. NO. OF REFS (total cited in document) 25
7. DESCRIPTIVE NOTES (the category of the document, e.g. technical report, technical note or memorandum. If appropriate, enter the type of report, e.g. interim, progress, summary, annual or final. Give the inclusive dates when a specific reporting period is covered). Technical Memorandum		
8. SPONSORING ACTIVITY (the name of the department project office or laboratory sponsoring the research and development. Include address). Defence R&D Canada – Ottawa 3701 Carling Avenue, Ottawa, Ontario, Canada K1A 0Z4		
9a. PROJECT NO. (the applicable research and development project number under which the document was written. Specify whether project). 15ec05	9b. GRANT OR CONTRACT NO. (if appropriate, the applicable number under which the document was written).	
10a. ORIGINATOR'S DOCUMENT NUMBER (the official document number by which the document is identified by the originating activity. This number must be unique.) DRDC Ottawa TM 2006-266	10b. OTHER DOCUMENT NOS. (Any other numbers which may be assigned this document either by the originator or by the sponsor.)	
11. DOCUMENT AVAILABILITY (any limitations on further dissemination of the document, other than those imposed by security classification) (X) Unlimited distribution () Defence departments and defence contractors; further distribution only as approved () Defence departments and Canadian defence contractors; further distribution only as approved () Government departments and agencies; further distribution only as approved () Defence departments; further distribution only as approved () Other (please specify):		
12. DOCUMENT ANNOUNCEMENT (any limitation to the bibliographic announcement of this document. This will normally correspond to the Document Availability (11). However, where further distribution beyond the audience specified in (11) is possible, a wider announcement audience may be selected).		

13. ABSTRACT (a brief and factual summary of the document. It may also appear elsewhere in the body of the document itself. It is highly desirable that the abstract of classified documents be unclassified. Each paragraph of the abstract shall begin with an indication of the security classification of the information in the paragraph (unless the document itself is unclassified) represented as (S), (C), (R), or (U). It is not necessary to include here abstracts in both official languages unless the text is bilingual).

Recently, there has been considerable interest in noise radar over a wide spectrum of applications, such as through wall surveillance, detection, tracking, Doppler estimation, polarimetry, interferometry, ground-penetrating or subsurface profiling, synthetic aperture radar (SAR) imaging, inverse synthetic aperture radar (ISAR) imaging, foliage penetration imaging, etc. One of the major advantages of the noise radar is its inherent immunity from jamming, detection, and external interference. In this report, the basic theory of noise radar design is treated. The theory supports the use of noise waveforms for radar detection and imaging in such applications as covert military surveillance and reconnaissance. It is shown that by using wide-band noise waveforms, one can achieve high resolution and reduced ambiguities in range and Doppler estimations. Two coherent processing receivers, namely, the correlation receiver and the double spectral processing receiver of noise radar returns are described and their range estimation is presented. Mutual interference and low probability of interception (LPI) capabilities of noise radar are also evaluated. The simulation results show the usefulness of the noise radar technology to improve on conventional radars.

14. KEYWORDS, DESCRIPTORS or IDENTIFIERS (technically meaningful terms or short phrases that characterize a document and could be helpful in cataloguing the document. They should be selected so that no security classification is required. Identifiers, such as equipment model designation, trade name, military project code name, geographic location may also be included. If possible keywords should be selected from a published thesaurus. e.g. Thesaurus of Engineering and Scientific Terms (TEST) and that thesaurus-identified. If it not possible to select indexing terms which are Unclassified, the classification of each should be indicated as with the title).

Noise Radar
Random Signal Radar
Noise Radar Technology
Correlation Receiver
Double Spectral Processing Receiver
Mutual Interference
Low Probability of Interception
Electronic Counter Counter Measure
Counter Electronic Support Measure
Ambiguity Function
Through Wall Surveillance
Ground-Penetrating Applications
Foliage Penetration

Defence R&D Canada

Canada's leader in Defence
and National Security
Science and Technology

R & D pour la défense Canada

Chef de file au Canada en matière
de science et de technologie pour
la défense et la sécurité nationale



www.drdc-rddc.gc.ca